Phytopathologia Mediterranea
The international journal of the
Mediterranean Phytopathological Union

Firenze University Press
www.fupress.com/pm

Research Papers

Discovery of signature peptides through proteomic approach as potential biomarkers for root wilt infection in coconut trees

Perumalla Aman JAYAKER[1], Sundararajan VINO[1], Subramanian BABU[2,*]

[1] *School of Bio Sciences and Technology, Vellore Institute of Technology, Vellore 632014, India*
[2] *VIT School of Agricultural Innovations and Advanced Learning (VAIAL), Vellore Institute of Technology, Vellore 632014, India*
*Corresponding author. E-mail: babu.s@vit.ac.in

Summary. Root wilt disease of coconut associated with phytoplasma presence is characterized by late symptoms in the field and hence disease detection has been challenging. Several attempts have been made in the past for detecting the infection, which included microscopic, histochemical, immuno assays and DNA based methods. However, the successful detection with precision and by a cost-effective simple assay is still not available. The current study used two-dimensional electrophoresis followed by mass spectrometric identification of the differentially or uniquely expressed proteins in the infected palms compared to healthy ones. Among the different proteins identified in the study, mannan endo-1,4-beta mannosidase and BTB/POZ domain and ankyrin repeat containing NPR2 proteins were selected. Bioinformatic analyses were carried out to characterize these proteins and the signature peptides with antigenic properties were determined. Biomarker protein structure prediction, homology modelling indicated the structure and function as well as uniqueness of these proteins. The sequences of these signature peptides are unique to these proteins and were found to be part of salicylic acid binding amino acid residues, thus involved in systemic acquired resistance against pathogens of plants. It is reported the procedure for obtaining signature peptides of potential biomarker proteins for detection of root wilt infection in coconut. The antibodies developed against these peptides would have more specificity for a precise detection of root wilt infection in coconut farms.

Keywords. Disease detection, phytoplasma, proteome biomarkers, root wilt, signature peptides.

Citation: Jayaker, P.A., Vino, S. & Babu, S. (2025). Discovery of signature peptides through proteomic approach as potential biomarkers for root wilt infection in coconut trees. *Phytopathologia Mediterranea* 64(2): 161-182. doi: 10.36253/phyto-15977

Accepted: May 1, 2025

Published: September 12, 2025

Data Availability Statement: All relevant data are within the paper and its Supporting Information files.

Competing Interests: The Author(s) declare(s) no conflict of interest.

Editor: Assunta Bertaccini, Alma Mater Studiorum, University of Bologna, Italy.

ORCID:
PAJ: 0009-0000-5526-1708
SV: 0000-0002-0015-8460
SB: 0000-0003-2781-7136

INTRODUCTION

India accounts 32% of global coconut production. The Karnataka, Tamil Nadu, Kerala, and Andhra Pradesh are the major coconut growing states in India. Among them root wilt disease was reported in Tamil Nadu and Kerala. Similar diseases in coconut palms are also reported in other countries worldwide and described by various other names, including Bogia coconut

syndrome in Papua New Guniea (Miyazaki *et al*., 2018), Weligama coconut leaf wilt in Sri Lanka, Lethal bronzing in Texas, and lethal yellowing in Africa and Caribbean (Gurr *et al*., 2016).

Root wilt disease of coconut is associated with the presence of phytoplasmas and verified to be transmitted by *Haplaxius crudus* in the America continent while other planthoppers were only reported as infected with phytopalsmas (Dollet *et al*., 2020; Humphries *et al*., 2021; Bahder *et al*., 2023; Paredes Tomas *et al*., 2023; Fernandez-Barrera *et al*., 2024). Infected trees exhibit yellowing of leaves, flaccidity, necrosis of leaflets. Roots and inflorescence as well as leaf are rotting. The unopened pale-yellow spindle leaves are particularly susceptible to the disease presence (Ramjegathesh *et al*., 2019).

Bahder *et al.* (2020) characterized the lethal bronzing disease progression in date palms as early, moderate, and late-stage symptoms based on canopy discoloration at respective stages. However, irrespective of the disease stage, they observed the phytoplasma titer to be low in the leaves and high in the base of the trunk. Soto *et al.* (2020) recorded a higher phytoplasma titer leading to leaf collapse within four months.

Diagnosis of root wilt infection in coconut has been challenging for more than three decades. Microscopic observation of phloem tissues of infected plants (Solomon *et al*., 1983; Navratil *et al*., 2009) and histochemical analysis (Abdulsalam *et al*., 1993) were reported. ELISA based detection of phytoplasma proteins was developed later (Sasikala *et al*., 2001, 2005). Although universal primers for PCR amplification of phytoplasma genomic region was developed by Ceramic-Zagorac and Hiruki (1996), and a quantitative PCR system to amplify specific rRNA has been reported (Manimekalai *et al*., 2011).

However, the success rate in PCR based method is low due to the non-specific amplification in the complex metagenome of tender leaf tissue from phytoplasma infected coconut trees. Rather than targeting the organism for detection, proteomics offers an alternative strategy to identify differentially expressed proteins in the infected tissues which could serve as biomarkers of infection. The differentially expressed proteins may include i) pathogen derived proteins and or ii) host proteins in response to pathogen infection. In the current study, such biomarker proteins were specifically identified in the proteome of infected leaf samples. Signature peptides which are unique to the protein and do not show homology with any other peptides of other proteins were also analyzed and identified to improve the specificity of the detection technique.

MATERIALS AND METHODS

Sample collection

The tender leaf tissues from crown region of healthy and root wilt infected coconut trees were collected from two different coconut growing regions of Tamil Nadu, India namely Pollachi and Vellore, which are in the extreme west and north of the state with a distance of 267 miles. In each of these districts, root wilt infected and uninfected farms were chosen for sample collection. In Pollachi, healthy leaf tissues were from 'Tall × Dwarf' variety trees cultivated in Aliyar village and infected leaf tissues were from 'Chowghat orange dwarf' variety trees cultivated in Zamin Uthukuli village which are 15 miles away. In Vellore region, infected and healthy samples were collected from Pallikonda and Brahmapuram villages respectively, which are 17 miles away. Tender leaf tissues from the crown region of ten coconut trees from healthy and infected farms were collected. All the samples were carried to the laboratory in polyethylene bags in ice container. The samples were surface sterilized using 70% ethanol and stored at -80°C.

PCR confirmation of infected and healthy samples

DNA was extracted from tissue samples using the modified CTAB method as described by de Silva *et al.* (2023). Nested PCR was performed using two sets of primers namely, P1/P7 primers (Deng and Hiruki, 1991; Schneider *et al*., 1995) for the first PCR and R16F2n/R16R2 (Lee *et al*., 1995; Gundersen and Lee, 1996) for the second PCR. The 20 µL reaction mixture contained 2 µL of template DNA, 0.5 µM of each primer, 200 µM of dNTP and 10 µL of 1× master mix (Ampliqon, Denmark) and nuclease free water. The PCR conditions for P1/P7 primers are: initial denaturation step for 2 min at 94°C, followed by 40 cycles for 30 s at 94°C, annealing at 53°C for 30 s and extension at 72°C for 1.5 min, and final extension at 72°C for 10 min. The conditions for the second round of PCR with R16F2n/R16R2 primers are the same except 50°C for 30 s and 72°C for 1 min, for annealing and extension respectively. PCR reactions were carried out in a thermal cycler (BioRad, Singapore). The amplicons were analyzed in 1% agarose gel and stained with ethidium bromide.

Extraction of proteins from coconut leaf tissues

Phenol-SDS method: One gram of leaf tissue was homogenized using mortar and pestle in the presence

of liquid nitrogen followed by 5 mL of extraction buffer (0.1 M Tris HCl (pH 7.5), 30% (w/v) sucrose, 2% (w/v) SDS). The resulted slurry was transferred to sterile centrifuge tubes and subjected to vortexing with intermittent cooling on ice for 5 min. Equal volume of tris saturated phenol was added and contents were mixed by inverting the tubes up and down and allowed to stand on ice for 10 min and centrifuged at 12,000 rpm for 15 min. The organic phase obtained on top was collected in a separate tube to which 4 volumes of 0.1 M ammonium acetate in methanol was added and mixed by inverting the tubes followed by overnight incubation at -20°C. Samples were further centrifuged at 12,000 rpm for 15 min and the pellet was dissolved in 80% acetone containing 0.07% DTT vortexed and centrifuged at 12,000 rpm for 15 min. Acetone wash was repeated two more times. The pellet was air dried and dissolved in the rehydration buffer (8 M Urea, 2% CHAPS, 50 mM DTT, 0.2% ampholyte, bromophenol blue 20 µL). After sonication at 40% power rate, 5 sec burst with 10 sec time interval and incubated at 4°C overnight. Contents were centrifuged at 12,000 rpm for 15 min and the supernatant obtained was retained and stored at -80°C until further use.

2-D-Gel electrophoresis, Mass Spectrometry, and annotation

The quantified protein concentrations were normalized to 100 µg using rehydration buffer and subjected to IPG strip rehydration and first-dimension electrophoresis in a Protean IEF unit (Biorad, USA). Focusing of strips were programmed as follows: 50 µA limit per strip; 250 V for 15 min; 4000 V for 2 h; 4000 V for 5 h (20,000 Vh); 500 V hold step. The strips were equilibrated with buffers I with DTT and buffer II with iodoacetamide (Babu *et al*., 2005). The strips were placed on polyacrylamide separating gels with a high range protein molecular weight marker. SDS-PAGE was carried out in 12% and 15% separating gels at a constant voltage of 50 V. The electrophoresis continued until the dye front reached the bottom of gel. The gels were stained overnight with Coomassie brilliant blue R-250 followed by silver stain. Gel images were compared using PD Quest software and spot intensity was quantified using ImageJ software. Differentially expressed protein spots were selectively excised and subjected to MALDI TOF/TOF Mass spectrometry analysis at Sandor Lifesciences-Hyderabad, India. The spectrum search was performed using Mascot against Swissport 2019_09 -*Veridiplantae* database and protein hits were obtained at p value <0.05 confidence.

The functional annotation of the identified proteins was performed using QuickGo online server and MapMan "Bin" ontology in Mercator pipeline Version 3.0. The Conserved Domain Database, a component of NCBI's Entrez was used to annotate protein sequences and the conserved domains of the proteins were predicted. The data was used to draw a domain graph using TBtools for visualization.

Protein selection and in silico *characterization*

The differentially expressed proteins were analyzed using protein sequence motif search tool (https://www.genome.jp/tools/motif/MOTIF.html) of Prosite and Pfam databases. Based on the literature search on role of these proteins during plant-phytoplasma interactions, BTB/POZ domain and ankyrin repeat-containing protein NPR2 and Mannan endo-1, 4-beta-mannosidase were selected as biomarkers for phytoplasma disease in coconut.

The template for the identified query proteins was obtained by performing database search using NCBI-blastp tool (BLAST: Basic Local Alignment Search Tool (nih.gov)) against standard protein database, with Viridiplantae/Green plants (taxid:33090) as organism name. The templates were selected with sequence similarity above 45%. Further the protein structure was predicted *via* template-based homology modelling using Swiss modeller (https://swissmodel.expasy.org/). The alpha fold predicted structure obtained from uniport (UniProt)were considered for the biomarker protein having homology cover less than 40%.

Identification of signature peptides and their antigenicity

With a long-term objective developing antibodies for detection of root wilt infection in coconut trees, unique peptides in the biomarker with antigenicity were identified. The biomarker protein sequence was used to find potent antigens and subunit vaccines using VaXiJen v 2.0 server (VaxiJen (ddg-pharmfac.net)). Whereas the allergenicity was predicted using AllerHunter server (http://allerdictor.vbi.vt.edu/). Further the linear B-cell epitope prediction using the Immune Epitope Database (IEDB) (http://tools.immuneepitope.org/bcell/) module of Kolaskar and Tongaonkar (Kolaskar and Tongaonkar, 1990) was employed. With 75% accuracy, the results predicted the epitopes. Additionally, the IEDB was used to predict the characteristics of B-cell epitopes, including the predictions of Emini surface accessibility, Parker, Karplus and Schulz flexibility, and Bepipred linear epitope. The results also supported Chou and Fasman's prediction that the antigenic portions of the

proteins are restricted to beta turn regions. For a comprehensive compression, B-cell epitopes were further predicted based on artificial neural network http://crdd.osdd.net/raghava/abcpred/ABC_submission.html and BepiPred-2.0 (Jespersen *et al*., 2017). Further, the B-cell continuous epitopes were predicted using secondary structure of biomarker proteins in PDB format as input in ElliPro server (http://tools.iedb.org/ellipro/). Using a support vector machine tool (http://sysbio.unl.edu/SVMTriP/prediction.php) the predicted linear epitopes having similar amino acids with a length ranging from 10-15 residues were selected. The epitopes were manually searched against Uniport protein database to validate them as signature peptides specific to the biomarker protein. All the analysis was performed under unaltered default settings.

RESULTS

Collection of root wilt infected and healthy coconut leaf samples

The samples are collected from two different districts based on the field survey and observation of symptoms of the disease. The healthy and root wilt infected coconut trees and the wilting symptom on the infected leaves are shown in Figure 1. To confirm the infected and healthy situation of the trees from which samples were collected for proteome analysis, DNA was extracted from the tissues and PCR was performed using the above listed primers targeting the 16S rRNA region of phytoplasma genome, under nested PCR conditions. The expected amplicon of 1800 bp from PCR was used as template for the nested PCR with R16F2n/R16R2 which resulted in an amplicon size of 1250 bp (results not shown).

Differentially expressed proteins

Out of the two protein extraction methods followed, phenol-SDS method resulted in higher protein concentration in the samples indicating the efficiency of extraction and solubilization. Hence, for all the samples, proteins extracted by phenol-SDS method was used for two-dimensional gel electrophoresis. The two-dimensional electrophoresis gel images of proteins solubilized from healthy and infected leaf tissues are presented in Figure 2. SBA is the label given to all the differentially expressed protein spots from another replication (gel images not shown). Among all these samples, the number of differentially expressed proteins were 8 in leaf tissues from healthy leaves and 21 in infected leaves. MALDI-TOF/TOF MS analysis revealed the identity of the proteins and are listed in Table 1.

Compared to the infected leaf samples, the most abundant proteins in healthy leaf samples includes ubiquitin protein transferase, magnesium dependent protein

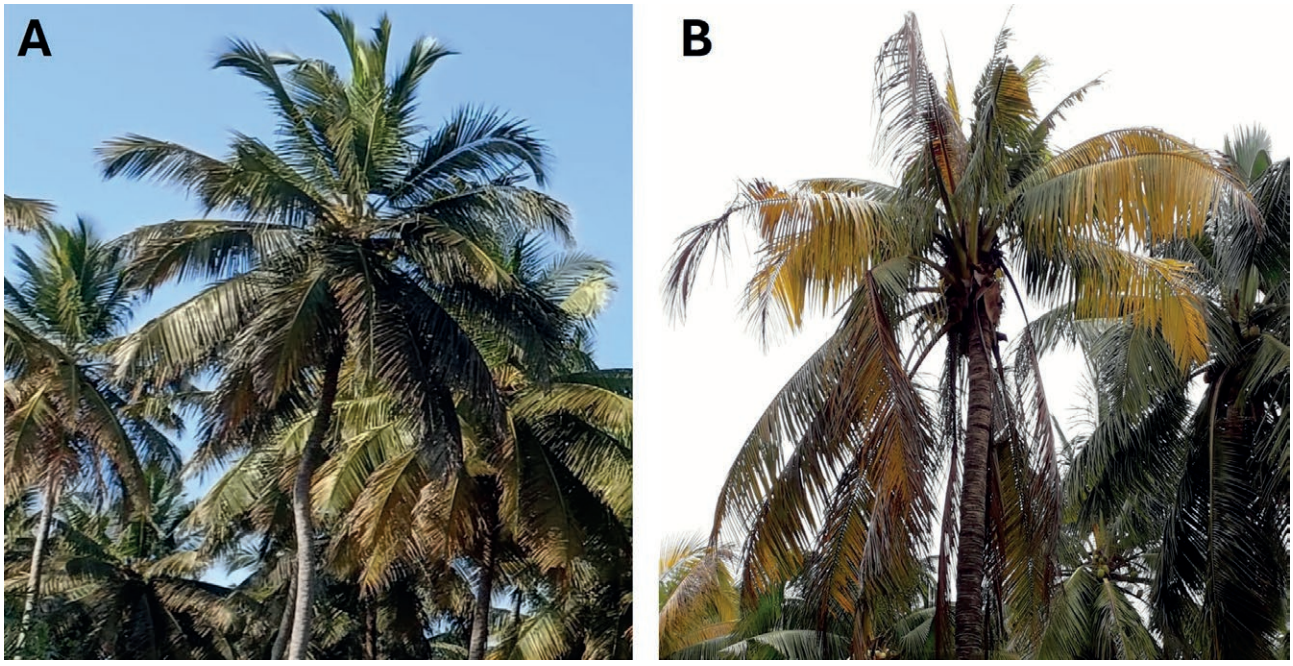

Figure 1. Field symptoms of root wilt infection in coconut. (A) Leaves of healthy coconut tree. (B) Leaves of root wilt infected coconut tree.

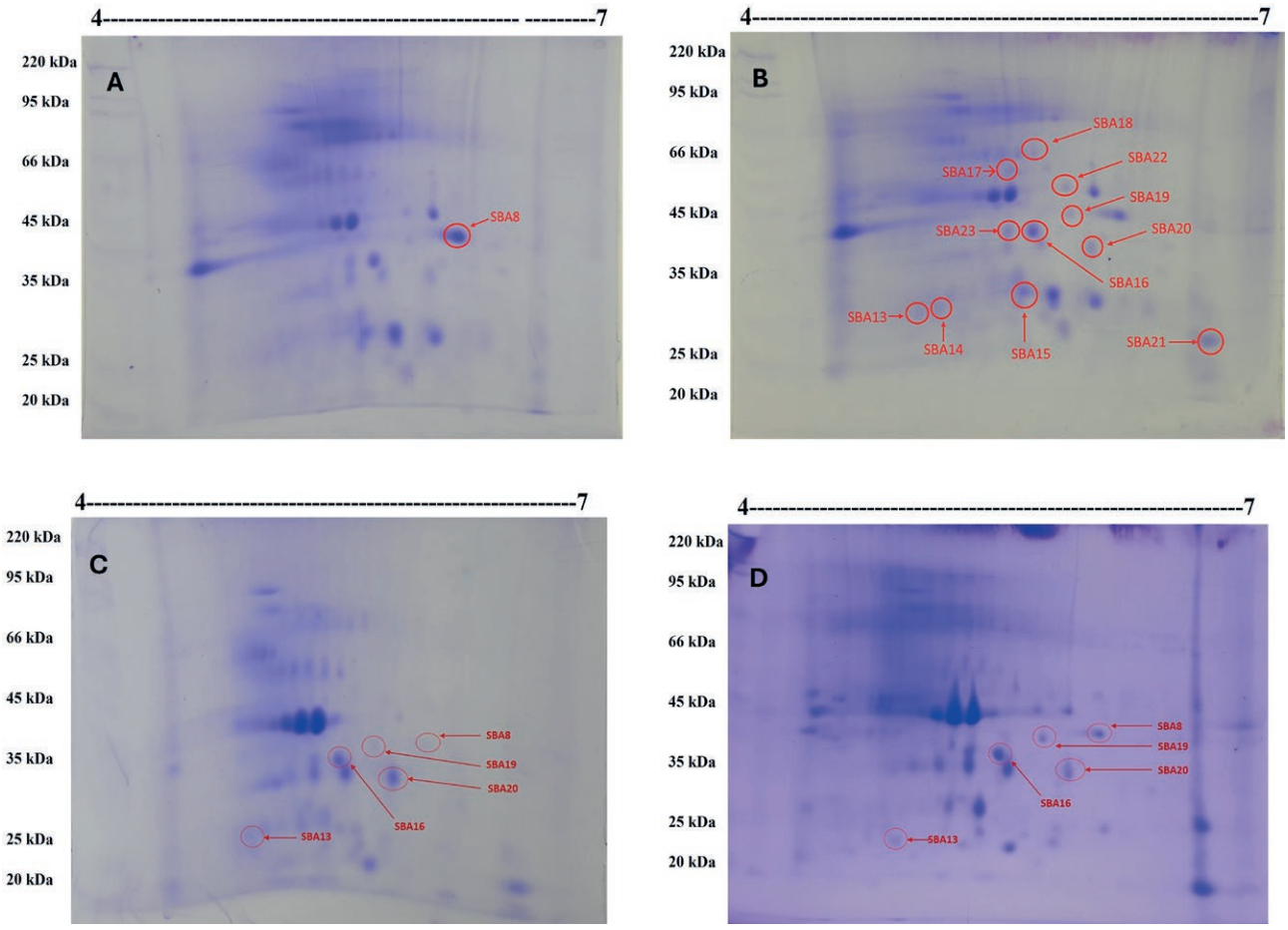

Figure 2. Two-dimensional electrophoretic analysis of healthy and infected coconut leaf proteome (Samples from Vellore and Pollachi, Tamil Nadu – Coommassie stained). (A) Leaf proteins from uninfected coconut trees. (B) Leaf proteins from root wilt infected coconut trees.

serine/threonine phosphatase, mannitol dehydrogenase, structural protein of cytoskeleton, co-localizing protein with bZIP18, in the nucleoplasm, GTPase activator and glycogen synthase, in addition to the house-keeping genes like DNA binding, RNA binding, photosynthesis, zinc ion binding. Table 1 reports the details of the mass spectrometry analysis.

The functional grouping of proteins (Figure 3) in the leaf tissues of healthy coconut trees indicated that 29% of proteins were found to be involved in protein modification, 20% in secondary metabolism, 10% in glycolysis, 10% in amino acid metabolism, 10% in cell wall organization and 26% in enzyme classification. In the leaf tissues of root wilt infected trees, 4% of proteins were found to be involved in processes like photosynthesis, glycolysis, nucleotide metabolism, DNA damage response, signaling, development, carbohydrate metabolism, stress response, C1-metabolism, and cell division. About 8% of proteins were related to hormone metabolism and RNA processing. About 12% were involved in protein modification and 20% in secondary metabolism. Among all identified proteins, homeobox-leucine zipper protein ROC4 was predicted as transcription factor responsible for drought resistance in rice. The majority of differentially expressed proteins were localised to cytoplasm followed by nucleus and chloroplast in both the root wilt infected and healthy coconut leaf samples (Figure 3).

Biomarker proteins

The conserved domains of all the identified proteins in both healthy and root wilt infected samples were predicted, which revealed the amino acid sequence associated with the predicted conserved domain cluster. The conserved domains of the differentially expressed proteins are presented in Figure 4. The amino acid residues not falling in any of the groups of conserved domain were used in identification of signature peptides. The two proteins *viz*., mannan endo-1, 4-beta-mannosidase and

Table 1. Differentially expressed proteins in healthy and root wilt infected coconut leaf tissues.

Protein ID	Accession No.	Protein	Peptides Matched	No. of peptides matched	Score	Sample type	On gel expression level	Molecular function	Experimental molecular mass (kDa)	Calculated molecular mass (kDa)	pI
SBA1	PUB73_ ORYSJ	U-box domain-containing protein 73 (*Oryza sativa Japonica* group)	K.AKADMSGLQR.S K.AKADMSGLQR.S R.MLDAGGMKMLR.G R.MLDAGGMKMLR.G R.QLSSDRLPMQK.M R.LTIILNLTMHR.Q K.NMEDFIERLR.Q R.LTIILNLTMHR.Q R.LPMQKMLQVER.I R.TLSDAFPAPTVRGR.C K.VASIVAVLSEFDMFR.K K.DTEVITEAATAILALYADGEGEQPAR.F	13	173	Healthy	Upregulating	Ubiquitin-protein transferase activity	36	64	4.80
SBA2	P2C44_ ORYSJ	Probable protein phosphatase 2C 44 *(Oryza sativa Japonica Group)*	K.DDISCIVIR.F K.ANLFCNILK.E K.DMWVANVGDSR.A+Oxidation (M) K.DDISCIVIRFR.C K.QLGPGGSTAVTAIVVDGK.D R.HVPINSSIEFVILASDGLWK.V R.AVVCERGAANQLTVDHEPHTTNER.Q	7	131	Healthy	Upregulating	Magnesium-dependent protein serine/threonine phosphatase activity	28	35	4.70
SBA3	MTDH_ MEDSA	Probable mannitol dehydrogenase (*Mucuna pruriens*)	K.YYGMTEPGK.H R.ENGDDDVSVK.I K.MHEINTAMER.L+2 Oxidation (M) K.HNITADIELIK.M -.MAKSPETELPLK.A K.ETQEMLDFCGK.H K.ETQEMLDFCGK.H+Oxidation (M) K.SPETELPLKAFGWAAR.D K.AFGWAARDTSGTLSPFHFSR.K K.LNGKLVTVGLPSKPLELSVFPLVAGR.K	10	142	Healthy	Upregulating	Mannitol dehydrogenase activity	32	39	5.00
SBA4	TBB2_ MAIZE	Tubulin beta-2 chain (*Zea mays*)	R.HGRYLTASAMFR.G+Oxidation (M) R.MMMTFSVFPSPK.V+2 Oxidation (M) R.LHFFMVGFAPLTSR.G+Oxidation (M) R.EILHIQGGQCGNQIGSK.F R.GLSMSSTFVGNSTSIQEMFR.R+2 Oxidation (M) R.EEYPDRMMMTFSVFPSPK.V+2 Oxidation (M) K.SSVCDIPPRGLSMSSTFVGNSTSIQEMFR.R+2 Oxidation (M)	7	61	Healthy	Upregulating	Structural constituent of cytoskeleton	34	50	5.10
SBA5	PP13_ TOBAC	Serine/threonine-protein phosphatase PP1 isoenzyme 3 (*Nicotiana sylvestris*)	IYGFYDECK IKYPENFFLLR QLCVASRDIFLK SSNPGKLVQLSESEIK QSLETICLLLAYKIK ILCMHGGLSPDLSSLDQIR NLPRPTAIPDTGLLCDLQRSDPGK	7	61	Healthy	Upregulating	Protein serine/_ threonine phosphatase activity	28	35	5.15

(Continued)

Table 1. (Continued).

Protein ID	Accession No.	Protein	Peptides Matched	No. of peptides matched	Score	Sample type	On gel expression level	Molecular function	Experimental molecular mass (kDa)	Calculated molecular mass (kDa)	pI
SBA6	NEAP1_ ARATH	Nuclear envelope-associated protein (*Arabidopsis thaliana*)	R.MTQLGHQLDDLQR.G+Oxidation (M) .MSYSEKTTVDPLLR.D R.DMEIKEIRDLISEK.Q+Oxidation (M) K.LVSQEQSFLKETITR.K K.IVVSMSMLMLVVVSKR.-+2 Oxidation (M) K.IVVSMSMLMLVVVSKR.-+3 Oxidation (M) K.IQCSMLKQQLDDKTR.S K.IQCSMLKQQLDDKTR.S+Oxidation (M) K.LLEDVSPMKFERMNR.L+2 Oxidation (M) R.MTQLGHQLDDLQRGLSLR.E+ Oxidation (M) R.EQEDRMTQLGHQLDDLQR.G K.AGIGGMDSELQKLLEDVSPMK.F+ Oxidation (M) K.AGIGGMDSELQKLLEDVSPMK.F+2 Oxidation (M) K.FWDNSGFKIVVSMSMLMLVVVSK.R K.FWDNSGFKIVVSMSMLMLVVVSK.R+2 Oxidation (M) K.FWDNSGFKIVVSMSMLMLVVVSK.R+3 Oxidation (M)	16	114	Healthy	Upregulating	Colocalized with bZIP18 in the nucleoplasm	23	39	5.08
SBA7	RGAP4_ ARATH	Rho GTPase-activating protein 4 (*Arabidopsis thaliana*)	R.EEEEEEEERSEK.E R.INGENGQEEYIREELNK.G R.APSASATVFGVSTESMQLSYDTR.G K.EESADEEEEECAESVELVDIKK.S K.SSQSCHFPSPSSSSSTSCGGGNDGSNR.D	5	100	Healthy	Upregulating	GTPase activator activity	18	49	6.40
SBA8	SSG1_ SOLTU	Granule-bound starch synthase 1, chloroplasctc/ amyloplastic (*Solanum tuberosum*)	K.NCMSEELSWKEPAK.K K.GMNLIFVGTEVGPWSK.T R.GVDRVFVDHPMFLEK.V R.GVDRVFVDHPMFLEK.V + Oxidation (M) K.EFEQEIEQLEVLYPNK.A K.GVAKFNVPLAHMITAGADFMLVPSR.F + Oxidation (M) K.GSDILVAAIHKFIGLDVQIVVLGTGK.K K.FNVPLAHMITAGADFMLVPSRFEPCGLIQLHAMR.Y + 2 Oxidation (M)	8	69	Healthy	Upregulating	Glycogen (starch) synthase activity	39	67	6.30
SBA9	FEN1_ OSTLU	Flap endonuclease 1 (*Ostreococcus lucimarinus)*	K.EHGSIEKILEEIDTEK.Y R.LESFFGPPTIISSTIGKR.K R.VAIDASMHIYQFMMVVGR.Q + Oxidation (M) R.ELFKNPEVMDTTGIALSWK.A R.RVAIDASMHIYQFMMVVGR.Q K.AGLVWAVATEDMDTLTFAAPRLAR.N + Oxidation (M) R.VAIDASMHIYQFMMVVGRQGEQQLTNEAGEVTSHLQGMLNR.T	7	101	Infected	Upregulating	magnesium ion binding	28	43	4.30
SBA10	DHSO_ ARATH	Sorbitol dehydrogenase (*Arabidopsis thaliana*)	R.MKAVGICGSDVHYLK.T + Oxidation (M) K.VCLVGMGHGIMTVPLTPAAAR.E + 2 Oxidation (M) R.AEVGPETNVLVMGAGPIGLVTMLAAR.A R.CGGKVCLVGMGHGIMTVPLTPAAAR.E + 2 Oxidation (M) K.GGMSQGEGSKVEEENMAAWLVGINTLK.I + 2 Oxidation (M) R.AEVGPETNVLVMGAGPIGLVTMLAARAFSVPR.A	6	92	Infected	Upregulating	oxidative activity	27	40	4.50

(Continued)

Table 1. (Continued).

Protein ID	Accession No.	Protein	Peptides Matched	No. of peptides matched	Score	Sample type	On gel expression level	Molecular function	Experimental molecular mass (kDa)	Calculated molecular mass (kDa)	pI
SBA12	TDC1_ ORYSJ	Tryotophan decarboxylase 1-like (*Oryza sativa Japonica* Group)	K.TGKAYVAHTVVGGR.F K.LWMVMRTYGVAK.L + Oxidation (M) R.SYLHKAVDFISDYYK.S R.FEVVVPRNFALVCFR.I R.ASPPTYSAPFDVTMKELR.S + Oxidation (M) K.NHASDSGEVTDLKDMQVGVGR.R K.WLMTCLDCTCLYVRDTHR.L R.LAGFDPANIRSIPTGAETDYGLDPAR.L	8	101	Infected	Upregulating	L-tryptophan decarboxylase activity	26	56	5.20
SBA13	Q0JJ01	BTB/POZ domain and ankyrin repeat-containing protein NPR2 *(Oryza sativa)*	K.EVDLNETPVTQNK.R R.RYFPNCSQVLDK.F R.STFFYNLFAARGR.G K.NSRGYTALHLAAMR.R K.SQPNEGDTVISDPVHEK.R K.SQPNEGDTVISDPVHEKR.V R.ADNSMFSILSSSSSSSPPPK.V R.ADNSMFSILSSSSSSSPPPK.V + Oxidation (M) K.VAMQIAQADTTPEFGIVPAASTSGK.L K.VAMQIAQADTTPEFGIVPAASTSGKLK.E R.EMIRKPMAVEDSVTSPLLADDLHMK.L	11	76.6	Infected	Upregulating	Salicylic acid signaling	39	69	5.9
SBA14	Q7Y0V9	Homeobox-leucine zipper protein ROC4 *(Oryza sativa)*	R.DQGITSASSTANMNCR.R R.DQGITSASSTANMNCR.R + Oxidation (M) K.LVGLTGNIGEDVHVMARK.S + Oxidation (M) K.QLADGVWAVVDVSADELMR.D + Oxidation (M) R.ESGIVIIDDGAALVETLMDER.R R.ESGIVIIDDGAALVETLMDERR.W	6	48.3	Infected	Upregulating	DNA-binding	25	87	6.5
SBA15	Q09FV4	ATP synthase subunit beta, chloroplastic (*Nandina domestica*)	R.TREGNDLYMEMK.E + Oxidation (M) R.INPTTSGPGVSALEEKNQGR.I K.GIYPAVDPLDSTSTMLQPR.I + Oxidation (M) R.GMEVIDTGAPLSVPVGGATLGR.I K.ELQDIIAILGLDELSEDDR.L R.MPSAVGYQPTLSTEMGSLQERITSTK.E + 2 Oxidation (M) K.MPNIYNALVVKGQDTVGQQINVTCEVQQLLGNNR.V	7	100	Infected	Upregulating	ATP binding	33	53	5.1
SBA16	Q9GI85	Maturase K *(Adesmia lanata)*	K.GLYRIK.Y R.MYQQNHLLLFANDSKK.N + Oxidation (M) R.QFISSLEDAETIKSFNNLR.S R.IKQLLSEHSFHFFWGGYISNVR.L	4	61	Infected	Upregulating	RNA-Binding	39	61	5.3
SBA17	D5JBX0	Germacrene A hydroxylase *(Helianthus annuus)*	K.LLTRPTSSKNR.L R.QAMNLAGYDVANKTK.L + Oxidation (M) R.ECRQAMNLAGYDVANK.T K.LDSLINNLVAEHTVSKSSK.V K.LPNGASHDQLDMTESFGATVQRK.T K.LPNGASHDQLDMTESFGATVQRK.T + Oxidation (M) R.LPIIGHMHHLIGTMPHRGVMDLAR.K + Oxidation (M) R.RMCPGSALGLANVQLPLANILYYFK.W + Oxidation (M)	8	80.5	Infected	Upregulating	heme binding	45	55	5.1

(Continued)

Table 1. (Continued).

Protein ID	Accession No.	Protein	Peptides Matched	No. of peptides matched	Score	Sample type	On gel expression level	Molecular function	Experimental molecular mass (kDa)	Calculated molecular mass (kDa)	pI
SBA18	Q8GVE8	Phosphoenolpyruvate carboxylase 4 (*Arabidopsis thaliana*)	R.IVLGEVK.E R.RDEDNNK.L K.QLTSEISK.M K.LFEESQVGK.T K.VHNVTQLAR.S R.QKPTPVDEAR.A K.MPLEEALTLAR.T + Oxidation (M) R.AGLNIVEQSLWK.A R.MAGIEDTANLLEK.Q + Oxidation (M) R.EVGNPFMEKVER.I R.EVGNPFMEKVER.I + Oxidation (M R.AIPWVFAWTQTR.F R.AHLPACIDFGESRHTK.F R.NLMEEISGISCQHYR.S + Oxidation (M) K.EVSLLSRWMAIDLYIR.E K.ELMTTEKYVLVISGHEK.L R.SGLTSRGSFSSTSQLLLQR.K R.VVPLFETVNDLRAAGPSIR.K K.DARLALTSEHGKPCPGGTLR.V R.HTKFEIATTDYMPPNLQK.Q + Oxidation (M) K.QNEQDFSESDWEKIDNGSR.S R.MAGIEDTANLLEKQLTSEISK.M + Oxidation (M) K.SSSGIGHLRAIPWVFAWTQTR.F R.ILAQSALNLRMAGIEDTANLLEK.Q + Oxidation (M) R.EHIQKNHNGHQEVMVGYSDSGK.D + Oxidation (M) K.FTGKPLPLTCTPMKFGSWMGGDR.D R.GGSIGRGGGPTYLAIQSQPPGSVMGSLR.S + Oxidation (M) R.HSEALDAITTYLDMGTYSEWDEEKK.L	28	130	Infected	Upregulating	phosphoenolpyruvate carboxylase activity	50	62	5.40
SBA19	Q8W2X5	Flavanone 3-dioxygenase 2 *(Oryza sativa)*	K.YRSVWHR.A K.LYSDDPAKK.I R.AVVNSDRER.M K.AKLYSDDPAK.K R.EFFRLPAEEK.A K.EIIGTYCTEVR.E R.MSVASFLCPCNSVELGPAK.K + Oxidation (M) R.MSVASFLCPCNSVELGPAKK.L + Oxidation (M) R.ERMSVASFLCPCNSVELGPAK.K .MAAEAEQQHQLLSTAVHDTMPGK.Y + Oxidation (M) K.WIAVNPQPGALVINIGDQLQALSNGK.Y R.THGFFQVVNHGIDAALIASVMEVGREFFR.L + Oxidation (M)	13	102	Infected	Upregulating	Dioxygenase activity	38	39	5.60

(Continued)

Table 1. (Continued).

Protein ID	Accession No.	Protein	Peptides Matched	No. of peptides matched	Score	Sample type	On gel expression level	Molecular function	Experimental molecular mass (kDa)	Calculated molecular mass (kDa)	pI
SBA20	F4JUY5	Gibberellic acid methyltransferase 1	R.YAVRAAADK.E K.GGVWIEGAEK.E K.DLVEFLKCR.K R.SLDEKVNGSSR.K K.YFAAGVPGSFYK.R K.RDGFNIPVYFR.T R.KYFAAGVPGSFYK.R K.SWNKGGVWIEGAEK.E R.LALSKPMLTTAINSIK.L + Oxidation (M) R.SLEHVLSMQGGEDDASYVK.N R.DGFNIPVYFRTTEEIAAAIDR.C R.ANYAQAGLKPIVQAYLGPDLTHK.L R.AAADKEILNNCFYHMIAVSAVR.V + Oxidation (M) K.NCYGPAARLALSKPMLTTAINSIK.L	7	55.5	Infected	Upregulating	gibberellin A9 carboxyl methyltransferase activity	36	18.7	5.70
SBA21	O65726	Squalene monooxygenase 1,2 *(Brassica napus)*	K.GLDEGSHIK.I R.NSIAPQVPLK.L R.QKASSLPNVR.L R.FFHNGRFVQR.L R.LLKPLGNLGDENK.V R.QGCFDYLSSGGFR.T K.ASSLPNVRLEEGTVR.S K.NLPSVSNGEMTSFVR.N + Oxidation (M) R.EPVRMMGEFMQPGGR.L + 2 Oxidation (M) K.AEGIGQMLSPTNAAAYR.K + Oxidation (M) R.MMGEFMQPGGRLMLSK.L K.EAMRQGCFDYLSSGGFR.T + Oxidation (M) R.MLLVFVLSWTIFHVNNRK.K + Oxidation (M) K.MLVPHLKAEGIGQMLSPTNAAAYR.K + Oxidation (M) K.NLPSVSNGEMTSFVRNSIAPQVPLK.L + Oxidation (M) R.KPMSATVNTLGNSFWQVLIASTDEAK.E + Oxidation (M) R.KPMSATVNTLGNSFWQVLIASTDEAKEAMR.Q + Oxidation (M)	17	100	Infected	Upregulating	Oxidoreductase	20	57	6.50
SBA22	P18026	Tubulin beta-2 chain *(Zea mays)*	R.MMMTFSVFPSPK.V + 2 Oxidation (M) R.LHFFMVGFAPLTSR.G + Oxidation (M) K.NSSYFVEWIPNNVK.S R.SLTVPELTQQMWDSK.N R.EILHIQGGQCGNQIGSK.F R.GLSMSSTFVGNSTSIQEMFR.R + 2 Oxidation (M) K.SSVCDIPPRGLSMSSTFVGNSTSIQEMFR.R + 2 Oxidation (M)	7	114	Infected	Upregulating	structural constituent of cytoskeleton	41	50	5.50

(Continued)

Table 1. (Continued).

Protein ID	Accession No.	Protein	Peptides Matched	No. of peptides matched	Score	Sample type	On gel expression level	Molecular function	Experimental molecular mass (kDa)	Calculated molecular mass (kDa)	pI
SBA23	A9RFQ5	Translation factor GUF1 homolog, chloroplastic *(Physcomitrella patens)*	K.FITENR.A R.GVVVYFR.V K.AANKGVDNGK.D K.IDLPGADPER.V K.VIASENIAAMRK.D R.NFSIIAHIDHGK.S K.AYSVGRALTQQLK.K R.SGSRYLHDLEAGR.S K.GYASMEYSVKGYR.E + Oxidation (M) R.EYGLDLITTAPSVVYR.V R.VDVPQDAFMAILRLEK.E + Oxidation (M) R.EIEEIIGLDCSEAILCSAK.E K.IPIQACIGSKVIASENIAAMR.K + Oxidation (M) R.REIEEIIGLDCSEAILCSAK.E	14	74.3	Infected	Upregulating	GTPase activity	30	82	5.10
SBA24	Q9FI48	Putative F-box protein (*Arabidopsis thaliana)*	K.ACLMSVNLHNHK.D + Oxidation (M) K.LMVWNPYLGQTR.W + Oxidation (M) K.IELNIVLWSKFLK.V K.KVAMVSELDIETCK.N + Oxidation (M) K.DNSKLMVWNPYLGQTR.W + Oxidation (M) -.MSTMSDLFPDLVEEILSR.V R.FYMGYDSNNNHKILWFSSMYR.E + 2 Oxidation (M) R.EEQLAVLFQKSDAYEMGIWITTK.I + Oxidation (M)	8	89.0	Infected	Upregulating	Unknown	39	44	5.90
SBSR10	Y1814_ ARATH	Uncharacterized Methyltransferase	K.NRGEK.K K.YAAQR.R R.QEIMR.Y R.VVFVSR.S K.EKLVLVR.A M.PMTVVSGR.F K.ACGLVNFTR.V K.NLRQEIMR.Y R.TPLVSFLYER.G	9	50	Healthy	Upregulating	methyltransferase activity	39	29	4.50
SBSR11	YCF4_ PELHO	Phytosystem I assembly protein	R.FLMK.D R.EIEQK.A R.RIFLR.F R.WGFPGR.N K.DIQSIR.I R.EGFYAR.R R.GQGAIPLTR.T K.EGIVCIFR.W R.IFLRFLMK.D	9	43	Infected	Upregulating	photosynthesis	21	66	5.00

(Continued)

Table 1. (Continued).

Protein ID	Accession No.	Protein	Peptides Matched	No. of peptides matched	Score	Sample type	On gel expression level	Molecular function	Experimental molecular mass (kDa)	Calculated molecular mass (kDa)	pI
SBSR12	MAN2_ ORYSJ	Mannan endo-1, 4-beta-mannosidase	K.VYLK.T R.LAAVR.Y R.QYVR.W K.FMTR.W K.SIDKK.H K.TLIMR.K R.DVLYR.A R.VSSMFR.T K.TLIMRK.N R.VSSMFRTAVSMGLTVCR.T	10	44	Infected	Upregulating	mannan endo-1,4-beta-mannosidase activity	50	44	5.30
SBSR13	CDA4_ ARATH	Probable inactive cytidine deaminase	M.TQQLK.F R.EEAASK.G K.FILTR.E R.ALTAANK.S K.SNAQYSK.C K.VSQEATAR.I R.APISGVQDAVLGLASSDR.I	7	51	Infected	Upregulating	zinc ion binding	27	33	5.70
SBSR14	PEN7_ ARATH	Putative pentacyclic triterpene synthase	R.SQYK.A K.KLIR.E R.HRTK.E K.QFPR.H K.EMLR.Y R.WPFK.K R.SMLIK.G R.GLVAAGK.T K.MDVER.L R.KEMLR.Y R.MQFLR.E K.WIIDR.G K.GYSFLR.K R.YIPIIK.N K.SACARAR.K R.GGATYTPLFGK.A K.TYQSYEPIR.R R.IMVDPDHDR.K	17	49	Infected	Upregulating	lanosterol synthase activity	89	27	5.90
SBSR15	YCF4_ CHLAT	Phytosystem I assembly protein	K.SDLIR.R K.AANLAR.F R.VIYLK.I K.EGINPR.R K.QDGIVR.I R.WGFPGK.N R.EIPLTR.I P.DPVLGSR.R K.SDLIRR.D K.EGINPRR.V R.VIYLKIK.G	11	62	Infected	Upregulating	photosynthesis	21	26	5.20

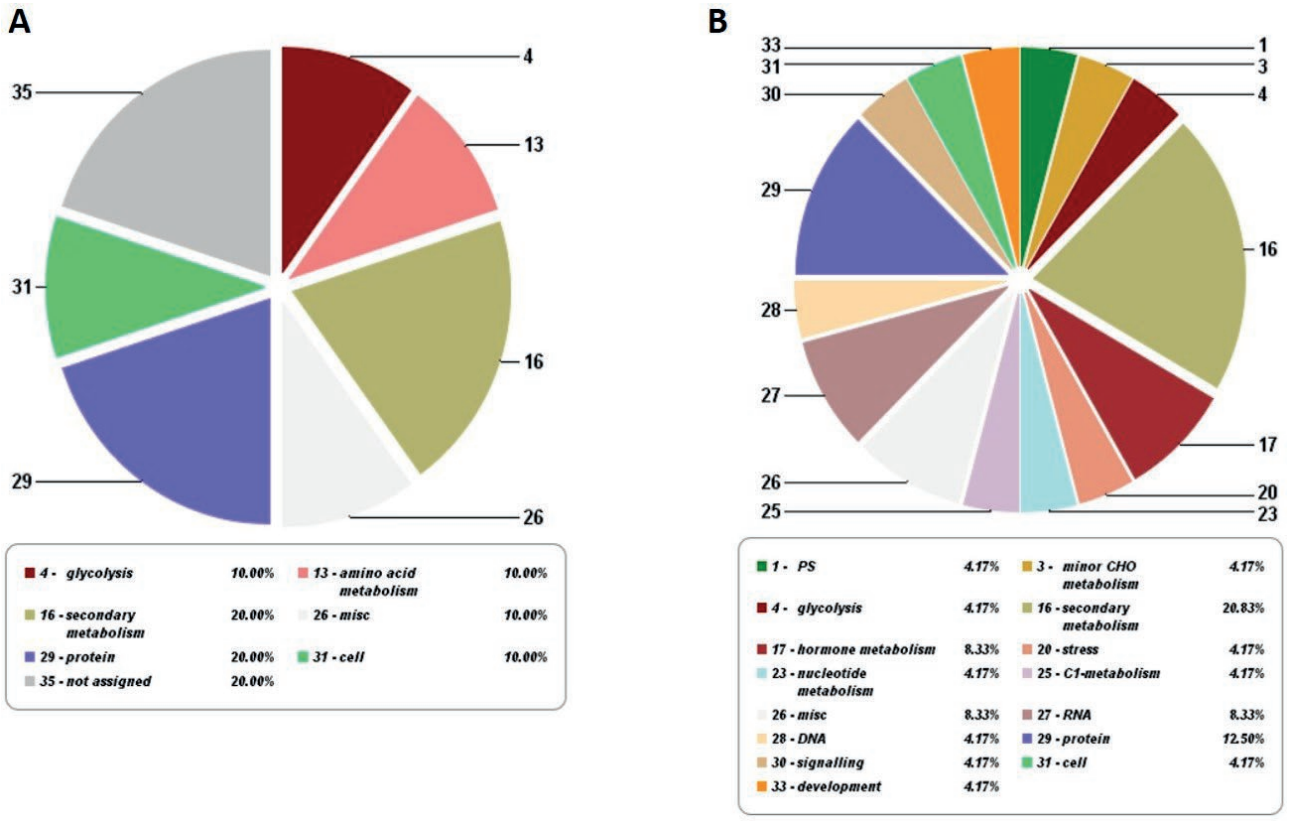

Figure 3. Functional classification of differentially expressed proteins in leaf tissues of coconut. (A) Leaf proteins from uninfected coconut trees. (B) Leaf proteins from root wilt infected coconut trees.

BTB/POZ domain and ankyrin repeat-containing protein NPR2 were selected as candidate biomarker proteins as they are functionally associated with phytoplasma infection in various plants. The conserved motifs in these potential biomarker proteins are presented in Figure 5.

The candidate protein sequence annotation, as determined by Prosite, revealed three motif profiles for the BTB/POZ ankyrin repeat protein: a circular ankyrin repeat region at amino acid positions 346-418, a BTB domain at positions 97-191, and an additional ankyrin repeat at positions 380-412. Pfam analysis disclosed six profiles for NPR1/NIM1-like defense protein C-terminal (422-626), domain of unknown function (276-323), ankyrin repeats (3 copies-323-407), multiple ankyrin repeats (350-392), ankyrin repeat (381-409), and BTB/POZ domain (97-194). The numbers indicate amino acid position in the protein sequence.

Gene ontology terms assigned by GO Central indicated the protein's involvement in defense responses to bacteria (GO:0042742), defense responses to fungi (GO:0050832), nuclear activity (GO:0005634), regulation of jasmonic acid-mediated signaling pathways (GO:2000022), and systemic acquired resistance mediated by salicylic acid signaling pathways (GO:0009862). Mercator annotation characterized its function as related to salicylic acid perception and signal transduction receptor protein (NPR3/4).

Furthermore, this study identified NPR-related peptides containing a conserved ethylene-responsive element-binding factor-associated amphipathic repression (EAR) motif sequence, notably VDLNE, which interacts with salicylic acid binding residues within NPR proteins such as VAMQIAQADTTPEFGIVPAASTSGK, TGKAYVAHTVVGGR, and RYFPNCSQVLDK. These residues have been reported to exhibit affinity towards salicylic acid. In our Mass spectrometry results (Table 1), the same peptides were observed in this BTB/POZ domain and ankyrin repeat-containing protein NPR2.

The biomarker protein mannan endo-1, 4-beta-mannosidase is functionally implicated in cell wall organization through modification and degradation facilitated by endo-beta-1, 4-mannanase activity on hemicellulose and heteromannan. Prosite profiling identified glycosyl hydrolases at amino acid positions 220-229, while Pfam

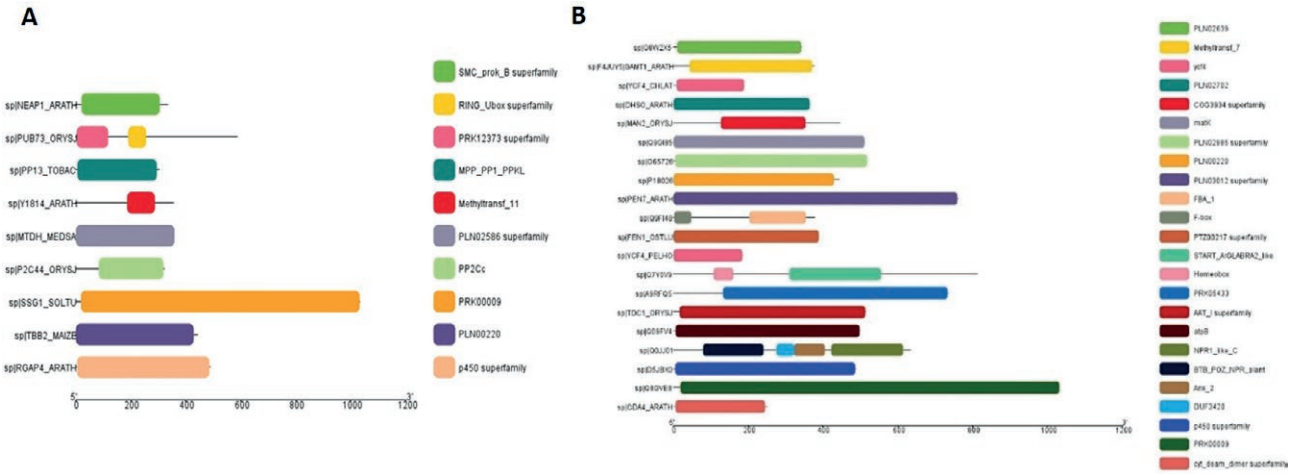

Figure 4. Conserved domains observed in the deferentially expressed coconut leaf proteins. (A) Leaf proteins from uninfected coconut trees. (B) Leaf proteins from root wilt infected coconut trees.

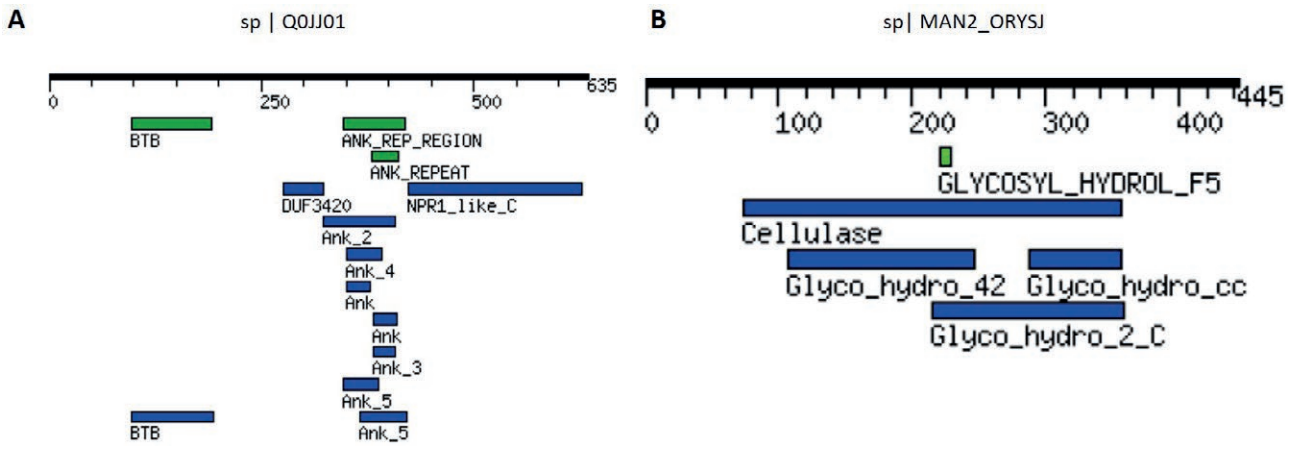

Figure 5. Conserved motif sites of the candidate biomarker proteins. (A) Leaf proteins from uninfected coconut trees. (B) Leaf proteins from root wilt infected coconut trees.

analysis detected cellulase (glycosyl hydrolase family 5 at positions 73-357, glycosyl hydrolase (288-357), beta-galactosidase (107-247), and glycosyl hydrolases family 2, TIM barrel domain family 5 signature (214-359).

Signature peptides and antigenicity

The biomarker protein sequences were subjected to BLAST searches against the NCBI-PDB database. The protein hit with the highest query coverage of 84% against endo-beta-mannanase (*Solanum lycopersicum*) (PDB ID: 1RH9_A) was selected and utilized as a template to build a model using SwissModel. However, for the biomarker protein containing the BTB/POZ domain and ankyrin repeats, the homology coverage was less than 40%. Therefore, the predicted structure from AlphaFold available in Uniprot was chosen instead.

The amino acid sequences of the selected biomarker proteins were submitted to the VaXiJen v 2.0 server, which aids in predicting potent antigens and subunit vaccines using default parameters, to determine antigenicity. Subsequently, the query sequences were screened against databases containing experimentally obtained antigenic residues (such as IEDB) along with various prediction modules (ABDpred, BepiPred-2.0, SVMTrip). Linear epitopes, as well as predictions for continuous and discontinuous epitopes were obtained from the analysis of the protein structure model using the Ellipro server. The predicted epitope sequences were

A

Bepipred Linear Epitope Prediction Average:0.491 Min:0.198 Max: 0.678		Kolaskar & Tongankar Antigenicity Average: 1.031 Min: 0.872 Min: 1.150		Parker Hydrophilicity Prediction Average: 1.752 Minimum: -2.386 Maximum: 5.907		Chou & Fasman Beta-Turn Prediction Average: 0.996 Min: 0.732 Max 1.541		Emini Surface Accessibility Prediction Average: 1.000 Min: 0.023 Max: 13.086		Karplus & Schulz Flexibility Prediction Average: 1.005 Min: 0.868 Max: 1.162		GRAVY score		Toxicity
Residue	Score	Peptide	Score	Peptide	Score	Peptide	Score	Peptide	Score	Peptide	Score	Peptide	Score	
V	0.439	HSELTPVLEKCIRR	1.065	HSELTPVLEKCIRR	1.207	HSELTPVLEKCIRR	0.899	SELTPVLEKCIR	0.351	LTPVLEK	1.004	V L E K C I R R I A R S N L	-0.007	N o n - T o x i n
L	0.429	SELTPVLEKCIRRI	1.069	SELTPVLEKCIRRI	0.486	SELTPVLEKCIRRI	0.865	ELTPVLEKCIRR	0.513	TPVLEKC	1.0			
E	0.434	ELTPVLEKCIRRIA	1.072	ELTPVLEKCIRRIA	0.171	ELTPVLEKCIRRIA	0.81	LTPVLEKCIRRI	0.208	PVLEKCI	0.991			
K	0.427	LTPVLEKCIRRIAR	1.074	LTPVLEKCIRRIAR	-0.086	LTPVLEKCIRRIAR	0.825	TPVLEKCIRRIA	0.254	VLEKCIR	0.983			
C	0.426	TPVLEKCIRRIARS	1.057	TPVLEKCIRRIAR	1.036	TPVLEKCIRRIARS	0.885	PVLEKCIRRIAR	0.345	LEKCIRR	0.972			
I	0.429	PVLEKCIRRIARSN	1.047	PVLEKCIRRIARSN	1.164	PVLEKCIRRIARSN	0.928	VLEKCIRRIARSN	0.299	EKCIRRI	0.965			
R	0.467	VLEKCIRRIARSNL	1.061	VLEKCIRRIARSNL	0.357	VLEKCIRRIARSNL	0.861	LEKCIRRIARSN	0.648	KCIRRIA	0.965			
R	0.478	LEKCIRRIARSNLD	1.024	LEKCIRRIARSNLD	1.336	LEKCIRRIARSNLD	0.93	EKCIRRIARSNL	0.648	CIRRIAR	0.966			
I	0.498	EKCIRRIARSNLDN	0.99	EKCIRRIARSNLDN	2.493	EKCIRRIARSNLDN	0.999	KCIRRIARSNLD	0.625	IRRIARS	0.979			
A	0.532	KCIRRIARSNLDNV	1.028	KCIRRIARSNLDNV	1.671	KCIRRIARSNLDNV	0.982	CIRRIARSNLDN	0.503	RRIARSN	0.998			
R	0.560	CIRRIARSNLDNVSL	1.034	CIRRIARSNLDNVSL	1.729	CIRRIARSNLDNVS	0.012	IRRIARSNLDNV	0.696	RIARSNL	1.016			
S	0.564	IRRIARSNLDNVSL	1.022	IRRIARSNLDNVSL	0.971	IRRIARSNLDNVSL	0.969	RRIARSNLDNVS	1.331	IARSNLD	1.037			
N	0.574	RRIARSNLDNVSLD	1.002	RRIARSNLDNVSLD	2.257	RRIARSNLDNVSLD	1.04	RIARSNLDNVSL	0.56	ARSNLDN	1.039			
L	0.577	RIARSNLDNVSLDK	1.006	RIARSNLDNVSLDK	2.364	RIARSNLDNVSLDK	1.044	IARSNLDNVSLD	0.478	RSNLDNV	1.032			

B

Figure 6. Characterization of epitopes and immunogenic residues in protein BTB/POZ domain and ankyrin repeat-containing protein. (A) Characterization of epitopes. (B) Homologous immunogenic residues plotted from various epitope predictions.

manually searched against non-conserved regions of the query protein. Further, epitopes with high homology across predicted results, with lengths ranging from 12 to 14 amino acid residues were retained. The results of the predictions for BTB/POZ domain and ankyrin repeat-containing protein NPR2 are presented in Figure 6 and for mannan endo-1, 4-beta-mannosidase protein in Figure 7. Additionally, the Uniprot peptide search revealed epitopes showing specific hits against the query biomarker proteins.

The Protein Localization Prediction Server (LocTree-Protter) was used to characterize the amino acid sequence of mannan endo-1, 4-beta-mannosidase. The topology and annotations showed a predicted epitope on the extracellular matrix. Similarly, for the BTB/POZ domain and ankyrin repeat-containing NPR2 protein, the prediction indicated localization within the intracellular matrix. Both proteins exhibited the N-glyco motif (Figure 8).

The signature peptides identified in the study for use as biomarkers in the molecular detection of root wilt infection in coconut are VLEKCIRRIARSNL and HQVEGFEDAHRD respectively for the BTB/POZ domain and ankyrin repeat-containing protein, and for mannan endo-1, 4-beta-mannosidase.

DISCUSSION

Root wilt disease is estimated to cause yield loss of up to 968 million nuts in South India (Manimekalai *et al.*, 2010). The Central Plantation Crops Research Institute of the Indian Council for Agricultural Research has associated the coconut root wilt disease in Tamil Nadu and Kerala states of India with the presence of phytoplasmas belonging to the 16SrXI group and also developed PCR detection techniques. They have also suggested some insect vectors involved in transmission of the disease such as lace bug and plant hoppers. ELISA based detection assay was also developed (https://cpcri.icar.gov.in).

Diagnosis of root wilt infection in coconut has been challenging for more than three decades. Microscopic techniques like fluorescent microscopy (Hibben *et al.*, 1986), electron microscopy (Solomon *et al.*, 1999) were

A

Bepipred Linear Epitope Prediction Average:0.482 Min:0.198 Max: 0.685			Kolaskar & Tongankar Antigenicity Average: 1.025 Min: 0.876 Max: 1.216		Parker Hydrophilicity Prediction Average: 1.155 Min: -3.075 Max: 5.708		Chou & Fasman Beta-Turn Prediction Average: 0.977 Min: 0.736 Max: 1.315		Emini Surface Accessibility Prediction Average: 1.000 Min: 0.077 Max: 6.384		Karplus & Schulz Flexibility Prediction Average: 0.987 Min: 0.888 Max: 1.134		Gravy Score		Toxicity
Position	Residue	Score	Peptide	Score	Peptide	Score	Peptide	Score	Peptide	Score	Peptide	Score	Peptide	Score	
353	H	0.522	GLSHQVE	1.07	EFGLSHQVEGFE	1.508	EFGLSHQVEGFE	0.916	LSHQVE	0.83	GLSHQVE	0.951	H		
354	Q	0.529	LSHQVEG	1.07	FGLSHQVEGFED	1.692	FGLSHQVEGFED	0.976	SHQVEG	0.996	LSHQVEG	0.962	Q		
355	V	0.558	SHQVEGF	1.047	GLSHQVEGFEDA	2.633	GLSHQVEGFEDA	0.981	HQVEGF	0.644	SHQVEGF	0.974	V		
356	E	0.578	HQVEGFE	1.024	LSHQVEGFEDAH	2.333	LSHQVEGFEDAH	0.93	QVEGFE	0.819	HQVEGFE	0.991	E		
357	G	0.595	QVEGFED	0.99	SHQVEGFEDAH	3.45	SHQVEGFEDAHR	0.96	VEGFED	0.79	QVEGFED	1.005	G		
358	F	0.593	VEGFEDA	0.997	HQVEGFEDAHRD	3.742	HQVEGFEDAHRD	0.962	EGFEDA	1.075	VEGFEDA	1.008	F	-1.6	Non-Toxin
359	E	0.578	EGFEDAH	0.957	QVEGFEDAHRDV	3.258	QVEGFEDAHRDV	0.925	GFEDAH	0.845	EGFEDAH	1.01	E		
360	D	0.579	GFEDAHR	0.961	VEGFEDAHRDVL	1.992	VEGFEDAHRDVL	0.893	FEDAHR	1.672	GFEDAHR	1.008	D		
361	A	0.561	FEDAHRD	0.959	EGFEDAHRDVLY	2.142	EGFEDAHRDVLY	0.946	EDAHRD	3.224	FEDAHRD	1.003	A		
362	H	0.529	EDAHRDV	1.001	GFEDAHRDVLYR	1.842	GFEDAHRDVLYR	0.963	DAHRDV	1.382	EDAHRDV	1.003	H		
363	R	0.517	DAHRDVL	1.058	FEDAHRDVLYRA	1.542	FEDAHRDVLYRA	0.888	AHRDVL	0.682	DAHRDVL	0.999	R		
364	D	0.509	AHRDVLY	1.1	EDAHRDVLYRAV	2.0	EDAHRDVLYRV	0.88	HRDVLY	1.058	AHRDVLY	0.99	D		

B

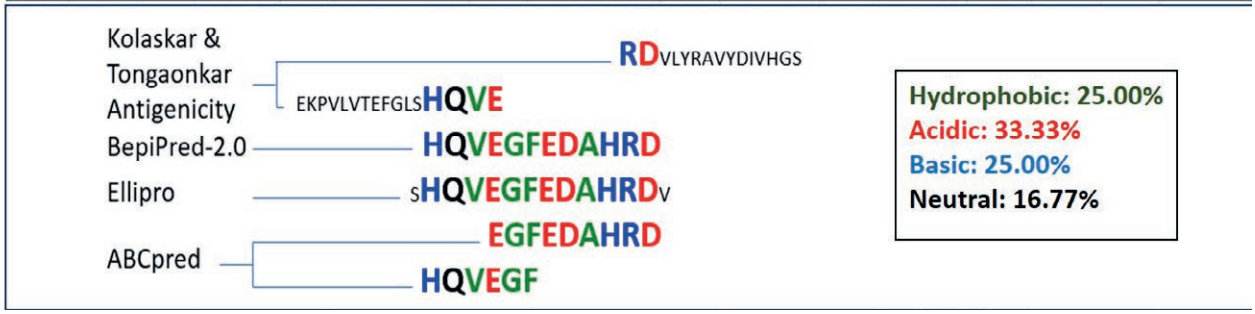

Figure 7. Characterization of epitopes and immunogenic residues in protein Mannan endo-1, 4-beta-mannosidase. (A) Characterization of epitopes. (B) Homologous immunogenic residues plotted from various epitope predictions.

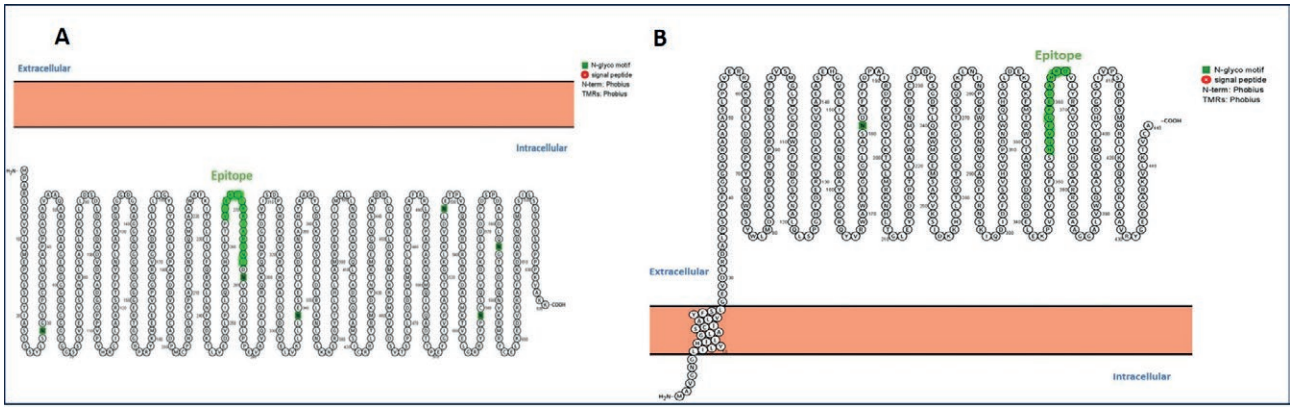

Figure 8. Graphical representation of biomarker proteins with predicted epitopes. A. Mannan endo-1, 4-beta-mannosidase protein sequence, topology and annotations depicts predicted epitope on intracellular matrix. B. BTB/POZ domain and ankyrin repeat-containing NPR2 protein sequence, topology and annotations depicts predicted epitope on intracellular matrix.

used in the past. Histochemical staining using 4,6, diamidino 2 phenylindole-2 hydroxychloride reaction indicated the presence of DNA in sieve tubes (Abdulsalam *et al.*, 1993). Thelly and Mohankumar (2001) observed lower H+ - ATPase in root wilt infected coconut leaves compared to healthy leaves and proposed H+ - ATPase as biochemical marker for early detection of the disease.

ELISA based detection of phytoplasmal proteins were developed later (Sasikala *et al.*, 2001). Due to the non-specificity that was observed in ELISA based detec-

tion, refinement of ELISA was done and used in the early detection of coconut wilt disease (Sasikala *et al*., 2005). Indirect ELISA using a polyclonal antibody was developed for detection of phytoplasma and it was reported to be capable of differentiating between phytoplasma-confirmed palms through PCR amplification of the phytoplasma-associated *secA* gene. (Kanatiwela-de Silva *et al*., 2019).

With the advent of PCR, universal primers for all phytoplasma were proposed (Ceramic-Zagorac and Hiruki, 1996) which was also used in detection of root wilt phytoplasma in coconut. The success was still 60% as the primers not always amplified the phytoplasma genomic region. The sample may consist of genomes of other microbes including viruses and bacteria in addition to the host genome. Homology of a few nucleotides in the 3' end of the primers in non-target DNA may mislead the output of the technique. Hence, nested-PCR was introduced (Lee *et al*., 1995) which made use of another set of genome specific primers and a second PCR reaction. This again consumed more time for detecting the presence of pathogen in the infected tissues but made the system more efficient.

In view of an improved detection strategy for phytoplasma associated coconut root wilt disease, Manimekalai *et al.* (2010) had developed a semi nested PCR primer pair observed no amplification in the healthy palm tissues which were asymptomatic. The same primer pair was used here to confirm the diseased and healthy coconut trees before proceeding to proteome analysis (Supplementary Figure 1). Similarly, this PCR analysis showed no amplification in asymptomatic tree samples except for two samples (Supplementary Figure 2). Nair *et al.* (2016) established a loop mediated isothermal amplification (LAMP) as a better method than conventional nested PCR. The infected samples resulted in ladder like bands, and the restriction digestion resulted in expected size fragments Ramjegathesh *et al.* (2019) developed qPCR assay combined with Taq Man probe. A 890 bp amplicon obtained from nested PCR was probed to specifically target a 69 bp region in 16S rRNA gene using Taq Man. Nested PCR followed by restriction analysis of 16S rRNA gene sequences was used to confirm Candidatus phytoplasma asteris group involved in the lethal wilt disease of coconut (Babu *et al*., 2021).

Instead of targeting a single gene (16S rRNA), targeting two genes including secA was used for detection of '*Candidatus* Phytoplasma palmicola' in Ecuatorial Guinea by Bertaccini *et al.* (2023) and '*Ca*. P. noviguineense' in Papua New Guinea by Dollet *et al.* (2022). De Silva *et al. (*2023) indicated in the nested PCR based detection that asymptomatic plants show no amplification. Hence, they optimized the primer pair combinations to result in 88 to 100% specificity in the detection of leaf wilt disease of coconut in Sri Lanka.

The two-dimensional electrophoresis is a high throughput analytical technique as it has potential in differentiating the proteome based on isoelectric point and molecular weight of individual proteins. The resulting differentially expressed proteins could be of pathogen origin in the infected tissues or host proteins produced in response to pathogen. Comparing the infected and uninfected coconut leaf tissues, it was possible to identify some differentially expressed proteins in replicated samples. Some of the previous studies on proteome analysis of plants infected with phytoplasma were successful in identifying the differentially expressed proteins indicating some of the proteins may be used as biomarkers for detection. Luge *et al.* (2014) identified defense related proteins and proteins involved in alpha-linoleic acid metabolism, that are upregulated in phytoplasma infected *Nicotiana occidentalis* plants. Cao *et al.* (2017) used transcriptome assisted proteomics in *Paulownia* seedlings infected with phytoplasma and identified many differentially expressed proteins with or without treatment using methyl methane sulfonate. By performing RT-qPCR, Margaria and Palmano (2011) correlated the protein expression level observed in proteome analysis of grapevine infected with phytoplasma, with the RNA concentration. Photosynthesis related proteins were found to be downregulated in plants infected with phytoplasma (Ji *et al*., 2009). However, in an iTRAQ quantitative proteomics study in *Ziziphus jujuba* – phytoplasma interaction, proteins involved in phenyl propanoid pathway and flavonoid biosynthesis were found to downregulated first and photosynthesis related proteins were downregulated later. This indicates that the phytoplasma downregulates the defence system of plants as the first thing during infection and later establishes to downregulate the photosynthesis. In another study, defense proteins were found to be induced in both susceptible and resistant varieties of Mexican lime infected with phytoplasma (Monavarfeshani *et al*., 2013). However, the time taken for the response in resistant plants was found to be less. Proteomics approach was used to identify candidate biomarkers for phytoplasma infection in sugarcane (Leetanasaksakul *et al*., 2022).

Previous reports on the role of some of the proteins observed in the present study are presented in Table 2. Tryptophan decarboxylase 1 – like protein was reported to play a role in disease resistance in rice plants against *Bipolaris oryzae*. Flavanone 3 – dioxygenase 2 is known for its role in plant interactions with phytoplasma and viruses. Putative penta cyclic triterpene synthase has been reported in Tanoak – Phytophthora interaction.

Table 2. Known roles of differentially expressed proteins in coconut trees under root wilt infection.

Protein ID	Accession No.	Protein Name	Superfamily	Expression	Plant-Pathogen	Reference
SBA12	tdc1_orysj	Tryptophan decarboxylase 1-like *Oryza sativa Japonica* Group	AAT_1 Aspartate aminotransferase	Upregulated upon infection showing resistance	*Oryza sativa -Bipolaris oryzae*	Ishihara *et al.*, 2011
				Over expressed TDC gene show resistance against whitefly	*Nicotiana – Bemisia tabaci*	Thomas *et al.*, 1995
SBA19	q8w2x5	Flavanone 3-dioxygenase 2 *Oryza sativa*	PLN02639 oxidoreductase	Flavonoid metabolism related protein upregulated upon infection	*Paulownia fortunei-'Candidatus* Phytoplasma asteris'	Wei *et al.*, 2017
					Vitis vinifera-"Flavescence dorée" phytoplasma	Margaria *et al.*, 2014
					Arabidopsis thaliana - Hyaloperonospora parasitica	Van Damme *et al.*, 2008
					Soybean mosaic virus resistance	Cheng *et al.*, 2010
SBSR14	pen7_arath	Putative pentacyclic triterpene synthase	PLN03012 Camelliol C synthase	Conserved amino acid residue aspartate "D" of DCTAE motif imply in β-amyrin synthesis	Oat	Salmon *et al.*, 2016
				Upregulated upon infection showing resistance	Tanoak - *Phytophthora ramorum*	Kasuga *et al.*, 2021
SBA20	F4JUY5	Gibberellic acid methyltransferase 1	SAM dependent carboxyl methyltransferase	Upregulated gene-Reduction in gibberellic acid levels	*Cocous nucifera*-Lethal yellowing phytoplasma	Nejat *et al.*, 2015
SBA13	q0jj01	BTB/POZ domain and ankyrin repeat-containing protein NPR2	NPR1_like_C/BTB_POZ_NPR_plant/ Ank_2/DUF3420	Upregulated NPR2 gene-Salicylic acid perception	*Arabidopsis thaliana- Pseudomonas syringae*	Dobón *et al.*, 2011
					Coconut-defense salicylic acid	Nic-Matos *et al.*, 2017
SBSR21	MAN2_ORYSJ	Mannan endo-1, 4-beta-mannosidase	COG3934 Glycoside hydrolase 5	Disease resistance	Wheat-*Fusarium graminearum/ Alternaria* sp.	Zhang *et al.*, 2020
					Transgenic tobacco-*Fusarium oxysporum*	Hoshikawa *et al.*, 2012
				Upregulated gene	Mexican lime trees- '*Candidatus* Phytoplasma aurantifolia=citri'	Mardi *et al.*, 2015
				Gene specifically expressed	Coconut-Lethal yellowing phytoplasma	Rajesh *et al.*, 2018
SBA14	q7y0v9	Homeobox-leucine zipper protein ROC4 *Oryza sativa*	Homeobox/ START_ArGLABRA2_like	Over expression	Rice-drought resistance/ Development of cuticular wax composition	Wang *et al.*, 2018

Three proteins such as gibberellic acid methyl transferase 1, BTB/POZ domain and ankyrin repeat containing protein NPR2 and mannan endo 1,4 mannosidase were previously reported in coconut – phytoplasma interaction and also in coconut salicylic acid defense pathway.

In the present study, mannan endo-1,4-beta mannosidase and BTB/POZ domain and ankyrin repeat containing NPR2 protein were identified as biomarker proteins for selection of signature peptides. Both were upregulated in the infected tissues. mannan endo-1,4-beta mannosidase is known to trigger defense against both fungal and bacterial pathogens in plants. Mannon oligosaccharides regulate stomata closure and cell death preventing the invasion of pathogens and also activate salicylic acid and jasmonic acid signaling pathways. BTB/POZ domain and ankyrin repeat containing NPR2 protein is a known activator of systemic acquired resistance (Boyle *et al*., 2009). Plant NPR1 and NPR2 are known to interact with promoter of pathogenesis related protein 1 (PR1) and NPR2 plays significant role in perception of salicylic acid (Canet *et al*., 2010; Backer *et al*., 2019). Both the proteins identified as potential biomarkers are well known in systemic acquired resistance in other plants.

Nevertheless, the protein biomarkers also have limitations due to their cross-reactivity of antibodies. Hence, after the identification of potential biomarker proteins through proteome analysis, bioinformatic analyses were carried out to identify the signature peptides. Signature peptides are unique tags of proteins and were initially developed for absolute quantification of a given protein in a mixture. Later, it was used for detection of a particular target protein (Geng *et al*., 2000). In both proteins under study, the signature peptides appeared to be part of salicylic acid binding residues, however the peptides are unique to each protein. The difference in peptide sequences also indicates that salicylic acid binding peptides are different between salicylic acid responsive proteins. The signature peptides to be conjugated with BSA or other carrier protein can be used for raising antibodies for further development of a simple lateral flow assay which will be useful for field level quick detection of coconut root wilt by immersing the strip in the sap obtained from the coconut crown leaves.

Since the proteins used to identify signature peptide biomarkers are upregulated proteins in infected symptomatic coconut trees, their upregulation in infected asymptomatic trees needs further evaluation. Hence the antibodies that would be developed using these signature peptides have to be tested in infected asymptomatic trees to develop them as biomarkers for early detection of the root wilt disease in coconut.

ACKNOWLEDGEMENTS

The authors gratefully acknowledge the Vellore Institute of Technology, Vellore, India for the support in providing the lab and field facilities to carry out the research. The funding support from Science and Engineering Research Board (SERB) of Department of Science and Technology, Government of India (SERB Sanction order no.: No.EMR/2017/000829) is gratefully acknowledged.

AUTHOR CONTRIBUTIONS

P.A.J: Methodology, Investigation, Formal Analysis, Data Curation, Writing Original Draft. S.V: Conceptualization, Methodology, Writing – Review and Editing, Supervision, Funding Acquisition. S.B: Conceptualization, Supervision, Project Administration, Writing – Review and Editing, Funding Acquisition.

LITERATURE CITED

Abdulsalam K.S., Abael-Mageed M.I., Resk M.A., Nageeb M.A., 1993. The influence of oxytetracycline on Wijamed date palm trees. *Annals of Agricultural Sciences* 38: 301–309.

Babu M., Thangeswari S., Josephrajkumar A., Krishnakumar V., Karthikeyan A., Karun A., 2021. First report on the association of '*Candidatus* Phytoplasma asteris' with lethal wilt disease of coconut (*Cocos nucifera* L.) in India. *Journal of General Plant Pathology* 87: 16–23.

Babu S., Bansal V.K., Kav N.N.V., 2005. Proteome-level investigation of *Brassica carinata*-derived resistance to *Leptosphaeria maculans*. *Journal of Agricultural and Food Chemistry* 53: 313–324.

Backer R., Naidoo S., van den Berg N., 2019. The nonexpressor of pathogenesis-related genes 1 (NPR1) and related family: mechanistic insights in plant disease resistance. *Frontiers in Plant Science* https://doi.org/10.3389/fpls.2019.00102.

Bahder B.W., Soto N., Mou D.F., Humphries A.R., Helmick E.E., 2020. Quantification and distribution of the 16SrIV-D phytoplasma in the wild date palm, *Phoenix sylvestris*, at different stages of decline using quantitative PCR (qPCR) analysis. *Plant Disease* 104: 1328–1334.

Bahder B.W., Zumbado Echavarria M.A., Barrantes Barrantes E.A., Helmick E.E., Bartlett C.R., 2023. A new species of planthopper in the genus *Shellenius*

(Hemiptera: Fulgoroidea: Derbidae) from palms in Costa Rica. *Zootaxa* 5306: 571–585.

Bertaccini A., Contaldo N., Feduzi G., Andeme A.M.E., Yankey E.N., Rovesti L., 2023. Molecular identification of '*Candidatus* phytoplasma palmicola' associated with coconut lethal yellowing in Equatorial Guinea. *Annals of Applied Biology* https://doi.org/10.1111/aab.12854.

Boyle P., Su E.L, Rochon A., Shearer H.L., Murmu J., Despres C., 2009. The BTB/POZ domain of the *Arabidopsis* disease resistance protein NPR1 interacts with the repression domain of TGA2 to negate its function. *Plant Cell* 21: 3700-3713.

Canet J.V., Dobon A., Roig A., Tornero P., 2010. Structure-function analysis of npr1 alleles in *Arabidopsis* reveals a role for its paralogs in the perception of salicylic acid. *Plant Cell and Environment* https://doi.org/10.1111/j.1365-3040.2010.02194.x.

Cao X., Fan G., Dong Y., Zhao Z., Deng M., Liu W., 2017. Proteome profiling of *Paulownia* seedlings infected with phytoplasma. *Frontiers in Plant Science* https://doi.org/10.3389/fpls.2017.00342.

Ceramic-Zagorac P., Hiruki C., 1996. Comparative molecular studies on aster yellows phytoplasmas. *Acta Horticulturae* 377: 266–276.

Cheng H., Yang H., Zhang D., Gai J., Yu D., 2010. Polymorphisms of soybean isoflavone synthase and flavanone 3-hydroxylase genes are associated with soybean mosaic virus resistance. *Molecular Breeding* 25: 13–24.

De Silva P.R., Perera C.N., Bahder B.W., Attanayake R.N., 2023. Nested PCR-based rapid detection of phytoplasma leaf wilt disease of coconut in Sri Lanka and systemic movement of the pathogen. *Pathogens* 12: 294.

Deng S.J., Hiruki C., 1991. Ampllification of 16s rRNA genes from culturable and nonculturable mollicutes. *Journal of Microbiological Methods* 14: 53–61.

Dobón A., Canet J.V., Perales L., Tornero P., 2011. Quantitative genetic analysis of salicylic acid perception in *Arabidopsis*. *Planta* 234: 671–684.

Dollet M., Fabre S., Beaumont M., Barnabe C., Namaliu Y., Bourdeix R., 2022. The phytoplasma associated with Bogia coconut syndrome in Papua New Guinea is a new phytoplasma in the group of the lethal yellowing syndromes (LYTS) of coconut and other palms. *Tropical Plant Pathology* 47: 530–552.

Dollet M., Fidelis E.G., Dos Passos E., Da Silva F., Aberlenc H.P, Bartlett C.R., 2020. Derbid planthoppers (Hemiptera: Fulgoroidea: Derbidae) associated with coconut and oil palm in Brazil. *Neotropical Entomology* 49: 722–738.

Fernández-Barrera M., Córdova-Lara I., Chan-Rodríguez J.L., Castillo-Vera A., Blanco-Rodríguez E., Saenz-Carbonell L., 2024. Detection of 16SrIV-A phytoplasma DNA in *Colpoptera* sp. (Hemiptera: Nogodinidae) insects in Yucatan Peninsula, Mexico. *Brazilian Journal of Biology* 84: 1–8.

Geng M., Ji J., Regnier F.E. 2000. Signature-peptide approach to detecting proteins in complex mixtures. *Journal of Chromatography A* 870: 295–313.

Gundersen D.E., Lee I-M., 1996. Ultrasensitive detection of phytoplasmas by nested-PCR assays using two universal primer pairs. *Phytopathologia Mediterrania* 35: 114–151.

Gurr G.M., Johnson A.C., Ash G.J, Wilson B.A.L., Ero M.M., You M.S., 2016. Coconut lethal yellowing diseases: A phytoplasma threat to palms of global economic and social significance. *Frontiers in Plant Science* 7: 1–21.

Hibben C.R., Lewis C.A., Castello J.D., 1986. Mycoplasma like organisms, cause lilac witches' broom. *Plant Disease* 70: 342–345.

Hoshikawa K., Endo S., Mizuniwa S., Makabe S., Takahashi H., Nakamura I., 2012. Transgenic tobacco plants expressing endo-β-mannanase gene from deep-sea *Bacillus* sp. JAMB-602 strain confer enhanced resistance against fungal pathogen (*Fusarium oxysporum*). *Plant Biotechnology Reports* 6: 243–250. https://doi.org/10.1007/s11816-012-0219-2.

Humphries A.R., Ascunce M.S., Goss E.M., Helmick E.E., Bartlett C.R., Bahder B.W., 2021. Genetic variability of *Haplaxius crudus*, based on the 5′ region of the cytochrome C oxidase subunit I gene, sheds light on epidemiology of palm lethal decline phytoplasmas. *PhytoFrontiers* 1: 127–134.

Ishihara A., Nakao T., Mashimo Y., Murai M., Ichimaru N., Miyagawa H., 2011. Probing the role of tryptophan-derived secondary metabolism in defense responses against *Bipolaris oryzae* infection in rice leaves by a suicide substrate of tryptophan decarboxylase. *Phytochemistry* 72: 7–13.

Jespersen M.C., Peters B., Nielsen M., Marcatili P., 2017. BepiPred-2.0: improving sequence based B-cell epitope prediction using conformational epitopes. *Nucleic Acid Research* 45: W24–W29. https://doi.org/10.1093/nar/gkx346.

Ji X., Gai Y., Zheng C., Mu Z., 2009. Comparative proteomic analysis provides new insights into mulberry dwarf responses in mulberry (*Morus alba* L.). *Proteomics* 9: 5328–5339.

Kanatiwela-de Silva C., Damayanthi M., de Silva N., Wijesekera R., Dickinson M., Udagama P., 2019. Immunological detection of the Weligama coconut

leaf wilt disease associated phytoplasma: Development and validation of a polyclonal antibody based indirect ELISA. *PLoS One* 14: 1–15.

Kasuga T., Hayden K.J., Eyre C.A., Croucher P.J.P., Schechter S., Garbelotto M., 2021. Innate resistance and phosphite treatment affect both the pathogen's and host's transcriptomes in the Tanoak – *Phytophora ramorum* pathosystem. *Journal of Fungi* 7: 198. https://doi.org/10.3390/jof7030198.

Kolaskar A.S., Tongaonkar P.C., 1990. A semi-empirical method for prediction of antigenic determinants on protein antigens. *FEBS Letters* 276: 172–174.

Lee I–M., Bertaccini A., Vibio M., Gundersen D.E., 1995. Detection of multiple phytoplasmas in perennial fruit trees with decline symptoms in Italy. *Phytopathology* 85: 728–735.

Leetanasaksakul K., Roytrakul S., Phaonakrop N., Kittisenachai S., Thaisakun S., Soulard L., 2022. Discovery of potential protein biomarkers associated with sugarcane white leaf disease susceptibility using a comparative proteomic approach. *Peer J* 10: e12740.

Luge T., Kube M., Freiwald A., Meierhofer D., Seeműller E., Sauer S., 2014. Transcriptomics assisted proteomic analysis of *Nicotiana occidentalis* infected by '*Candidatus* Phytoplasma mali' strain AT. *Proteomics* 14: 1882–1889.

Manimekalai R., Nair S., Soumya V.P., Roshna O.M., Thomas G.V., 2011. Real-time PCR technique-based detection of coconut root (wilt) phytoplasma. *Current Science* 101: 1209–1212.

Manimekalai R., Soumya V.P., Sathish Kumar R., Selvarajan R., Reddy K., Baranwal V.K., 2010. Molecular detection of 16SrXI group phytoplasma associated with root (wilt) disease of coconut (*Cocos nucifera*) in India. *Plant Disease* 94: 636–636.

Mardi M., Karimi Farsad L., Gharechahi J., Salekdeh G.H., 2015. In-Depth Transcriptome sequencing of Mexican lime trees infected with *Candidatus* phytoplasma aurantifolia. *PLoS One* 10: e0130425. https://doi.org/10.1371/journal.pone.0130425.

Margaria P., Ferrandino A., Caciagli P., Kedrina O., Schubert A., Palmano S., 2014. Metabolic and transcript analysis of the flavonoid pathway in diseased and recovered N ebbiolo and B arbera grapevines (*Vitis vinifera* L.) following infection by F lavescence dorée phytoplasma. *Plant Cell and Environment* 37: 2183–2200. https://doi.org/10.1111/pce.12332.

Margaria P., Palmano S., 2011. Response of the *Vitis vinifera* L. cv. 'Nebbiolo' proteome to "flavescence dorée" phytoplasma infection. *Proteomics* 11: 212–224.

Miyazaki A., Shigaki T., Koinuma H., Iwabuchi N., Rauka G.B., Namba S., 2018. '*Candidatus* phytoplasma noviguineense', a novel taxon associated with bogia coconut syndrome and banana wilt disease on the island of New Guinea. *International Journal of Systematic and Evolutionary Microbiology* 68: 170–175.

Monavarfeshani A., Mirzaei M., Sarhadi E., Amirkhani A., Nekouei M.K., Salekdeh G.H., 2013. Shotgun proteomic analysis of the Mexican Lime tree infected with '*Candidatus* Phytoplasma aurantifolia'. *Journal of Proteome Research* 12: 785–795.

Nair S., Manimekalai R., Raj P.G., Hedge V., 2016. Loop mediated isothermal amplification (LAMP) assay for detection of coconut root wilt disease and arecanut yellow leaf disease phytoplasma. *World Journal of Microbiology and Biotechnology* 32: 108.

Navratil M., Safarova D., Valova P., Franova J., Simkova M., 2009. Phytoplasma associated with witches'-broom disease of *Ulmus minor* MILL. in the Czech Republic: Electron microscopy and molecular characterization. *Folia Microbiologia* 54: 37–42.

Nejat N., Cahill D.M., Vadamalai G., Ziemann M., Rookes J., Naderali N., 2015. Transcriptomics-based analysis using RNA-Seq of the coconut (*Cocos nucifera*) leaf in response to yellow decline phytoplasma infection. *Molecular Genetics and Genomics* 290: 1899–1910. https://doi.org/10.1007/s00438-015-1046-2.

Nic-Matos G., Narváez M., Peraza-Echeverría S., Saenz L., Oropeza C., 2017. Molecular cloning of two novel *NPR1* homologue genes in coconut palm and analysis of their expression in response to the plant defense hormone salicylic acid. *Genes and Genomics* 39: 1007–1019.https://doi.org/10.1007/s13258-017-0566-z.

Paredes-Tomás C., Luis-Pantoja M., Rodríguez-Tapia J.L., Bertaccini A., 2023. *Haplaxius crudus* transmission of '*Candidatus* Phytoplasma palmae' to coconut seedlings in Cuba. *Phytopathogenic Mollicutes* 13: 151–156.

Rajesh M.K., Rachana K.E., Kulkarni K., Sahu B.B., Thomas R.J., Karun A., 2018. Comparative transcriptome profiling of healthy and diseased Chowghat Green dwarf coconut palms from root (wilt) disease hot spots. *European Journal of Plant Pathology* 151: 173–193.

Ramjegathesh R., Karthikeyan G., Balachandar D., Ramaraju K., Rajendran L., Samiyappan R., 2019. Nested and TaqMan ® probe based quantitative PCR for the diagnosis of '*Ca*. Phytoplasma' in coconut palms. *Molecular Biology Reports* 46: 479–488.

Salmon M., Thimmappa R.B., Minto R.E., Melton R.E., Hughes R.K., Osbourn A., 2016. A conserved amino acid residue critical for product and substrate speci-

ficity in plant triterpene synthases. *Proceedings of the National Academy of Sciences USA* 113: E4407–4414. https://doi.org/10.1073/pnas.1605509113.

Sasikala M., Chithra K.R., Solomon J.J., Rajeev G., 2001. Development of DAC Indirect ELISA for the rapid detection of coconut root (wilt) disease. *Coconut Research and Development Journal* 17: 34.

Sasikala M., Prakash V.R., Sapna V.P., Mayilvaganan M., Nair L.S., 2005. Refinement of ELISA and its use in early detection of coconut root (wilt) disease. *Coconut Research and Development Journal* 21: 37–44.

Schneider B., Seemüller E., Smart C.D., Kirkpatrick B.C., 1995. Phylogenetic classification of plant pathogenic mycoplasma-like organisms or Phytoplasmas. In: Razin S., Tully J.G., Eds., Molecular and Diagnostic Procedures in Mycoplasmology, Vol. I. Academic Press, San Diego, 369–380. http://dx.doi.org/10.1016/B978-012583805-4/50040-6

Solomon J.J., Govindankutty M.P., Nienhaus F., 1983. Association of mycoplasma-like organisms with the coconut root (wilt) disease in India. *Journal of Plant Diseases and Protection* 90: 295–297.

Solomon J.J., Nair C.P.R., Srinivasan N., Gunasekaran M., Sasikala M., 1999. Coconut root (wilt) – The malady and remedy. *Journal of Plantation Crops* 27: 71–92.

Soto N., Humphries A.R., Mou D.F., Helmick E.E., Glover J.P., Bahder B.W., 2020. Effect of oxytetracycline-hydrochloride on phytoplasma titer and symptom progression of the 16SrIV-D phytoplasma in cabbage palms from Florida. *Plant Disease* 104: 2330–2337.

Thelly T.M., Mohankumar C., 2001. H+-ATPase as a biochemical marker for early detection of root (wilt) disease in coconut palms (*Cocos nucifera* L.). *Indian Journal of Biochemistry and Biophysics* 38: 199–202.

Thomas J.C., Adams D.G., Nessler C.L., Brown J.K. and Bohnert H.J., 1995. Tryptophan decarboxylase, tryptamine and reproduction of the whitefly (*Bemisia tabaci*). *Plant Physiology* 109: 717–720.

Van Damme M., Huibers R. P., Elberse J., Van den Ackerveken G., 2008. Arabidopsis *DMR6* encodes a putative 2OG-Fe(II) oxygenase that is defense-associated but required for susceptibility to downy mildew. *The Plant Journal*. https://doi.org/10.1111/j.1365-313X.2008.03427.x.

Wang Z., Tian X., Zhao Q., Liu Z., Li X., Bu Q., 2018. The E3 ligase DROUGHT HYPERSENSITIVE negatively regulates cuticular wax biosynthesis by promoting the degradation of transcription factor ROC4 in rice. *Plant Cell* 30: 228–244. https://doi.org/10.1105/tpc.17.00823.

Wei Z., Wang Z., Li X., Zhao Z., Deng M., Dong Y., Fan G., 2017. Comparative proteomic analysis of *Paulownia fortunei* response to phytoplasma infection with dimethyl sulfate treatment. *International Journal of Genomics* 1–11. 10. https://doi.org/1155/2017/6542075.

Zhang S.B., Zhang W.J., Li N., Zhai H-C., Lv Y-Y., Cai J-P., 2020. Functional expression and characterization of an endo-1,4-β-mannosidase from *Triticum aestivum* in *Pichia pastoris*. *Biologia* 75: 2073–2081. https://doi.org/10.2478/s11756-020-00525-8.